Geophysical Research Letters

Supporting Information for

Reconsidering the relationship between Gulf Stream transport and dynamic sea level at U.S. East Coast

Lequan Chi[a], Christopher L.P. Wolfe[b] and Sultan Hameed[b]

[a]Skidaway Institute of Oceanography, University of Georgia, Savannah, GA 31411

[b]School of Marine and Atmospheric Sciences, Stony Brook University, Stony Brook, NY 11790

Corresponding author: Lequan Chi (Lequan.Chi@uga.edu)

Contents of this file

Introduction

Text S1 introduces how the monthly GS transport is derived from along-track altimetry. Text S2 discusses local wind effects on gridded sea level from altimetry. Table S1 lists details of tide gauges adopted in this study. Figure S1 & Figure S2 show monthly Florida Current transport (FCT) derived from different subsamples of its daily records. Figure S3 and Figure S4 show correlations between Gulf Stream transport at different locations for seasonal and annual means. Figure S5 (Figure S6) shows dominant wind direction at each tide gauge (grid point) derived by regressing vector wind vector against sea level. Figure S7 shows regression coefficients between alongshore wind stress and sea level at tide gauges. Figure S8 is similar to Figure 3, but show additional altimetry tracks. Figure S9 and Figure S10 are similar to Figure 3, but effects from local wind are removed. Figure S11 shows how sea level in the open ocean is correlated with

mean sea level at tide gauges. Figure S12 to Figure S16 repeat some calculations with global mean sea level removed. Note that linear trends are not removed from Figure S12 to Figure S16.

Text S1: Gulf Stream Transport from Along-track Altimetry

The Gulf Stream (GS) transport used in this study is derived by the following steps:

(a) Identify Gulf Stream axis

Frequently, eddies around the GS are accompanied by comparable velocity, making it difficult to distingush the GS from eddies by maximum downstream velocity. To exclude influences from the eddies, the 25-cm absolute dynamic topograhpy (ADT) contour from gridded weekly altimetry is adopted as the first guess of the GS position. Only the contour which extends continuously back to the Straits of Florida is used. This ADT contour has been shown to be good proxy for the GS path and is widely used by previous studies (e.g., Andres et al., 2013; Chi et al., 2019; Lillibridge and Mariano, 2013; Rossby et al., 2014). Since the GS axis so defined extends continuously back to the Straits of Florida, it provides an objective method to distingish the GS from the eddies surrounding it. At each satellite track, the GS axis is defined as the position of the maximum downstream velocity within 75 km of the 25-cm ADT contour. Chi et al. (2021) showed that the GS position derived from the above method is consistent to GS position from ADCP measurements at the Oleander Line (marked in Figure 1), in which influences from GS rings have been removed manually.

(b) Monthly Gulf Stream Transport

The cross-track surface velocity (v) is derveid based on the geostrophic balance:

$$v = \frac{g}{f}\frac{\partial h}{\partial x} \tag{S1}$$

where f is the Coriolis parameter, g is the gravitational acceleration, h is ADT and x is along-track distance (positive offshore). Transport is calculated each time the satellite crosses the GS (~10 days) by integrating the geostrophic velocity between the first point where it drops to zero north and south of the GS axis in the raw data. Given that v is propotional to sea level graident (Eq S1), the transport, T, is related to the cross-stream sea level drop, Δh, by

$$T = \frac{g}{f}\Delta h\,. \tag{S2}$$

GS transport is first interpolated into a daily timeseries by linear interpolation. Then, the monthly mean GS transport is derived by averaging the daily transports in each month. Even though the above GS transport only reflects the surface-layer transport, Rossby et al. (2010, 2005) showed that it is proportional to the depth-integrated GS transport. Rossby et al. (2014) evaluated the upper 2000-meter GS transport via multiplying its transport at ~55 m by a conatant value of 700.

(c) Evaluation of potential errors in GS transport due to sampling frequence

In this section, we use Florida Current trasnport (FCT) as an example to evaluate the reliability of monthly mean GS transport derived from samples separated by 10-day intervals, which is approximately the repeat period of the satellite altimetry used in this study. First, daily FCT time series measured by underwater cables are subsampled into 10-day intervals. Then the subsampled FCT is interpolated into a daily time series and subsequently averaged into monthly means the same way we derive monthly GS transport from satellite altimetry. We repeated the above procedures 11 times with different initial dates (Jan 1st, 2nd, … 11th, 1993), and generated 11 sets of monthly FCT time series, FCT_{s01}, FCT_{s02}, …, FCT_{s11}, correspondingly. $FCT_{s01}$is selected as the referenced time series and correlations between it and the monthly FCTs reconstructed from subsampling (FCT_{s01}, FCT_{s02}, …, FCT_{s11}) are shown in Figure S1. The results are approximately symmetrical about the 5-day lag. Even though the correlations drop with lags from 1 to 5 days, the minimal correlation, ~0.77 at the 5-day lag, is still much higher than correlations between FCT at neighboring tracks downstream of Cape Hatteras (below 0.25 as shown in Figure 2). Thus, the rapid decorrelation of GS transport with distance shown in Figure 2 is not likely to be due to the sampling frequency of satellite altimetry.

To further evaluate how well 3 records per month represents monthly FCT, Figure S2 shows correlations between the monthly FCT derived from all available daily measurements and the FCT derived from 3 records per month (FCT_{s01}, FCT_{s02}, …, FCT_{s11}). The correlations are about 0.93, which indicates that the monthly FCT derived from 3 records per month represents ~86.5% of the total variance. The above results suggest that monthly mean GS transport can be estimated reasonably well at the sampling frequency of satellite altimetry, though not perfectly.

Text S2: Local wind effects on sea level

Following Piecuch et al. (2019), we decompose sea level into a local wind-driven component and a residual component. First, the wind direction explaining the largest fraction of local sea level variance is determined by linearly regressing the local wind stress vector against sea level; then, sea level is regressed against wind stress in that direction. Figure S5 shows that the sea level at all the tide gauges is significantly correlated with the local wind stress. The direction of greatest correlation is approximately alongshore at most tide gauges (Figure S5) and on the shelf (Figure S6), consistent with Sandstrom (1980) and Piecuch et al. (2019).

On the shelf (shallower than 200 m), sea level from both tide gauges and altimetry is highly correlated with alongshore wind (Figure S5 and Figure S6) due to the existence of a lateral boundary (the coastline) and the Coriolis term (Piecuch et al., 2019; Sandstrom, 1980). Off the shelf, the wind stress is absorbed by the Ekman transport and does not directly affect sea level (Figure S6). Instead, sea level in the deep ocean respond when the Ekman transport converges or diverges due to the wind stress curl. We account for these different dynamics by estimating local wind effects in two different ways. For tide gauges and on the shelf (shallower than 200 m), sea level is regressed against longshore wind stress, while off the shelf, sea level is regressed against the wind stress curl. Note that the local wind effects are **not** removed from the sea level used to calculate Gulf Stream transport, just from the sea level used in the correlation analysis.

Station ID	Station Name	Longitude	Latitude	Completeness	Region
392	PORT AUX BASQUES	59.13	47.57	91.98%	CC
393	ST. JOHN'S, NFLD.	52.72	47.57	98.77%	CC
1299	NORTH SYDNEY	60.25	46.22	98.46%	CC
332	EASTPORT	66.98	44.90	96.60%	GoM
1158	YARMOUTH	66.13	43.83	94.75%	GoM
183	PORTLAND (MAINE)	70.25	43.66	99.69%	GoM
235	BOSTON	71.05	42.35	96.60%	GoM
351	NEWPORT	71.33	41.51	99.69%	MAB
1111	NANTUCKET ISLAND	70.10	41.29	97.22%	MAB
12	NEW YORK (THE BATTERY)	74.01	40.70	97.84%	MAB
180	ATLANTIC CITY	74.42	39.36	94.44%	MAB
1153	CAPE MAY	74.96	38.97	99.69%	MAB
1635	CHESAPEAKE BAY BR. TUN.	76.11	36.97	91.05%	MAB
1636	DUCK PIER OUTSIDE	75.75	36.18	96.91%	MAB
396	WILMINGTON	77.95	34.23	99.07%	SAB
1444	SPRINGMAID PIER	78.92	33.66	93.21%	SAB
234	CHARLESTON I	79.93	32.78	100.00%	SAB
395	FORT PULASKI	80.90	32.03	98.77%	SAB
112	FERNANDINA BEACH	81.47	30.67	91.67%	SAB
2123	TRIDENT PIER, PORT CANAVERAL	80.59	28.42	92.28%	SAB
1858	VIRGINIA KEY, FL	80.16	25.73	94.75%	SAB
188	KEY WEST	81.81	24.56	99.38%	SAB

Table S1: Details of tide gauges used in this study. “Completeness” is derived from the monthly mean records between 1993 and 2019. The regions SAB, MAB, GoM and CC refer to the South Atlantic Bight, the Middle Atlantic Bight, the Gulf of Maine, and the Canadian coast, respectively. Station Yarmonth is located in Canada but within the GoM.

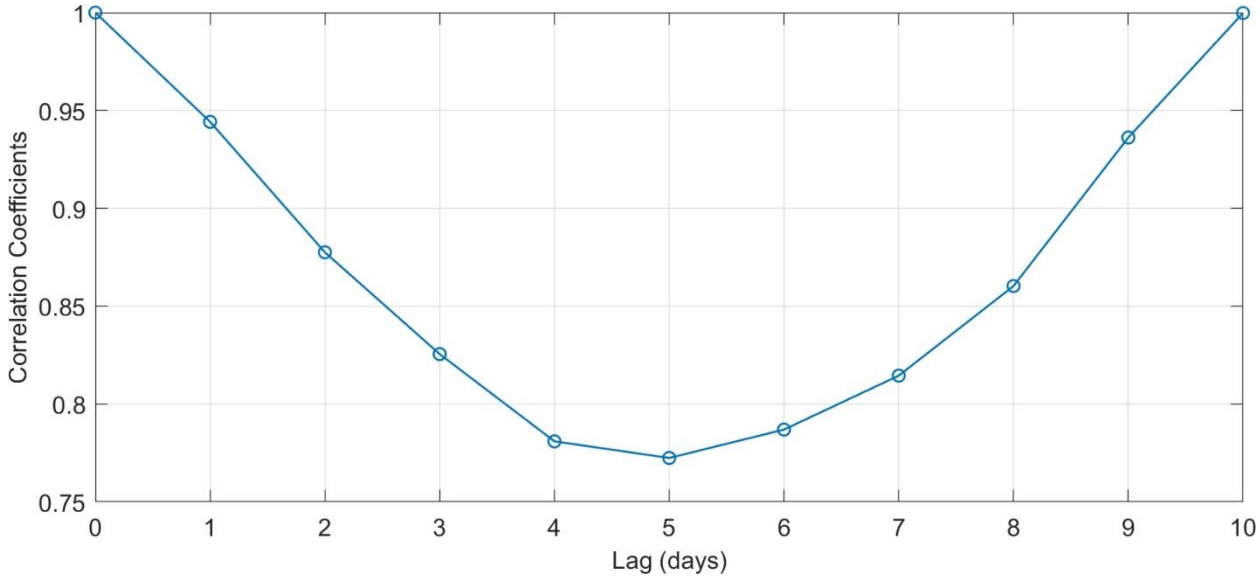

Figure S1: Correlations between monthly Florida Current transport (FCT) derived from daily FCT subsampled at 10-day intervals. The horizontal axis indicates lags between the initial dates in subsampling. All the correlations are significant at 99% confidence interval.

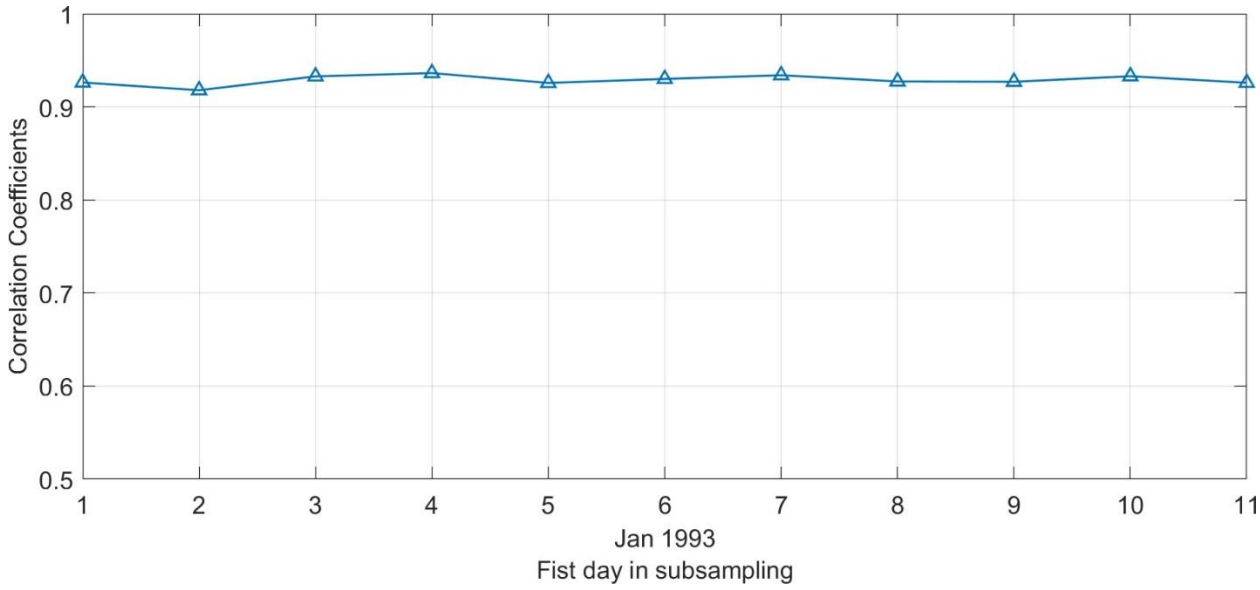

Figure S2: Correlation between monthly FCT derived from all available daily observations via underwater cables and monthly FCT reconstructed from subsampled FCT with 10-day intervals, FCT_{s01}, FCT_{s02}, …, FCT_{s11}. All the correlations are significant at 99% confidence interval.

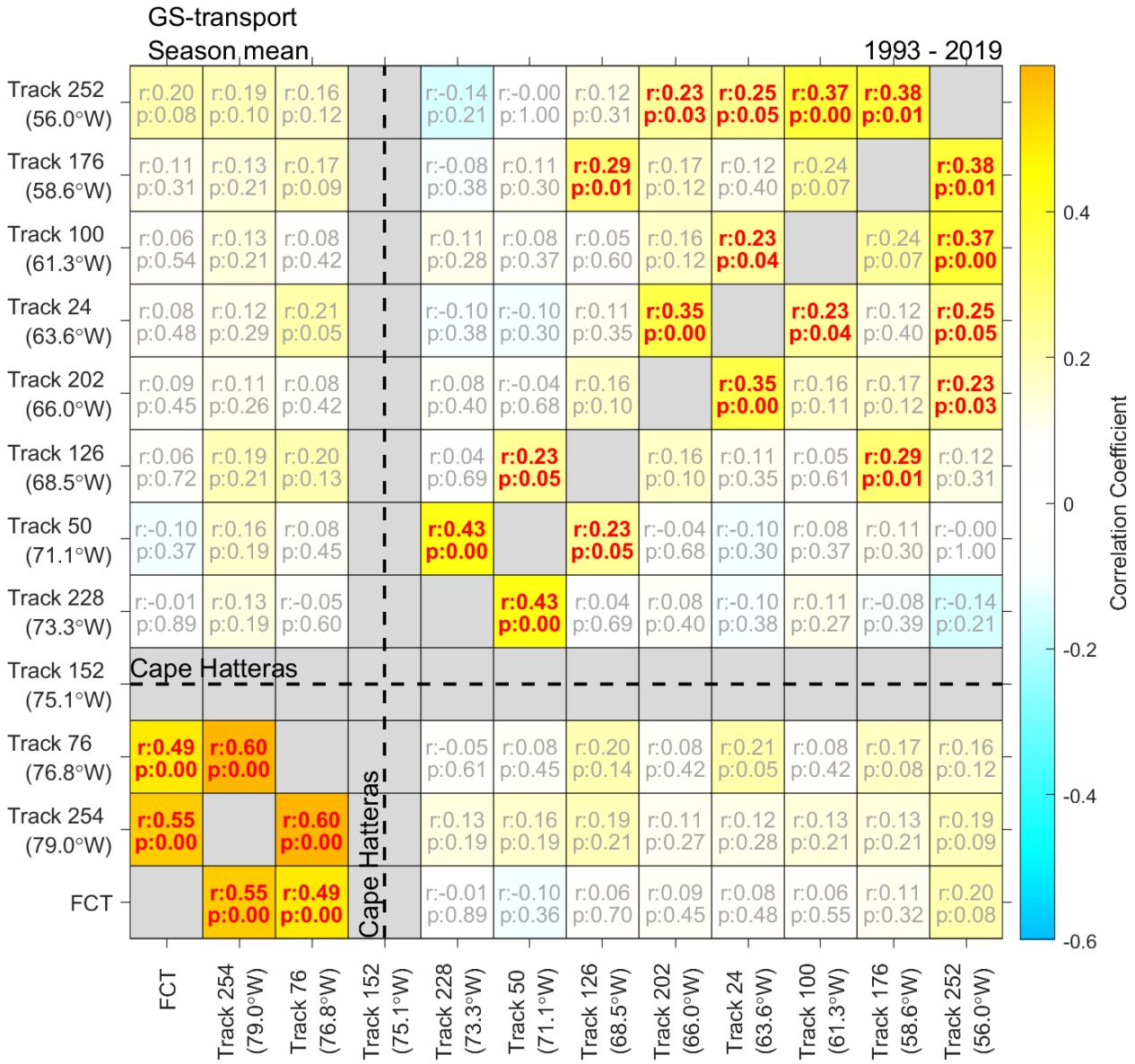

Figure S3: Same as Figure 2 but for seasonal mean GS transport, in which winter is defined as January-February-March (JFM)

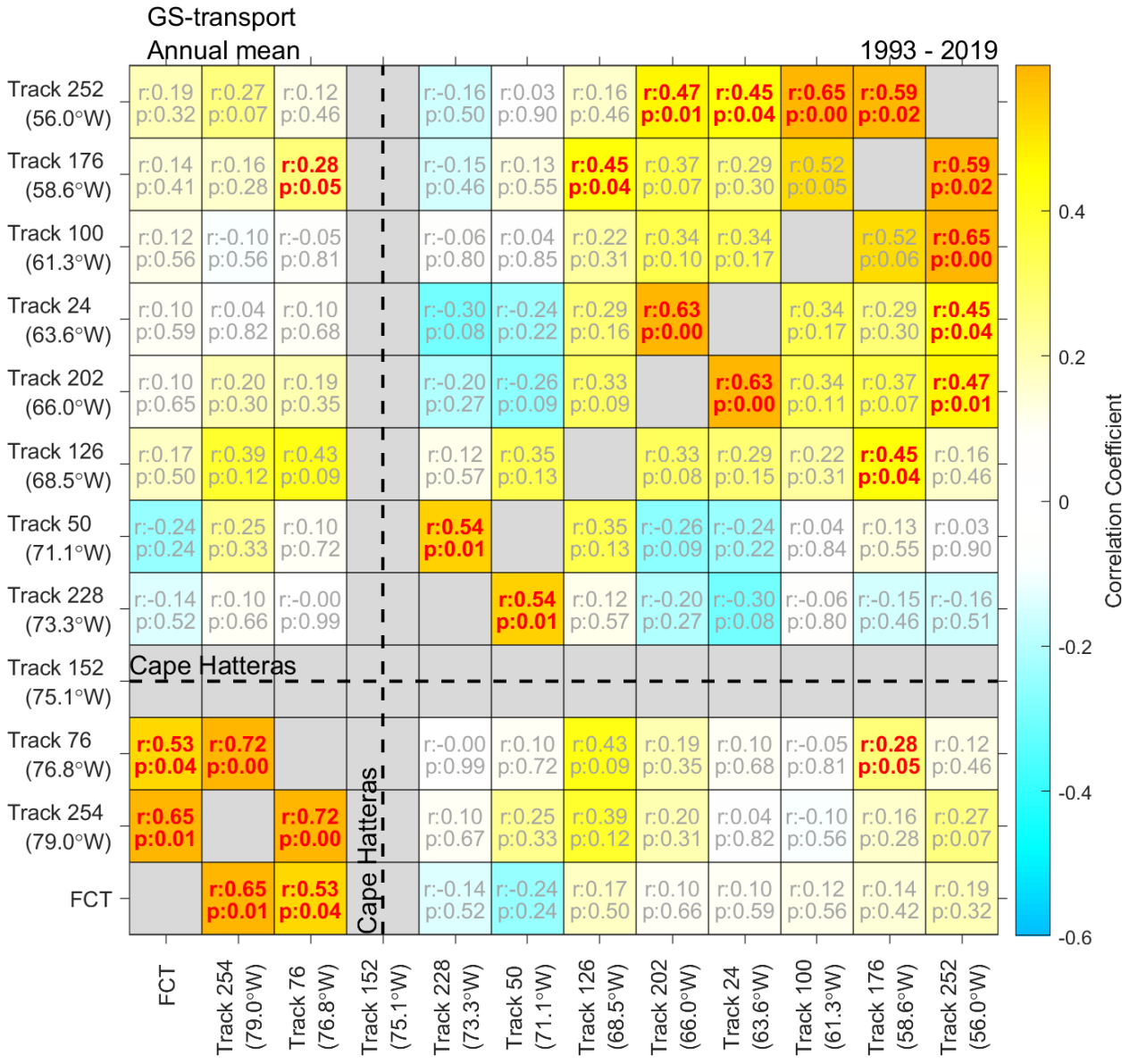

Figure S4: Same as Figure 2 but for annual mean GS transport.

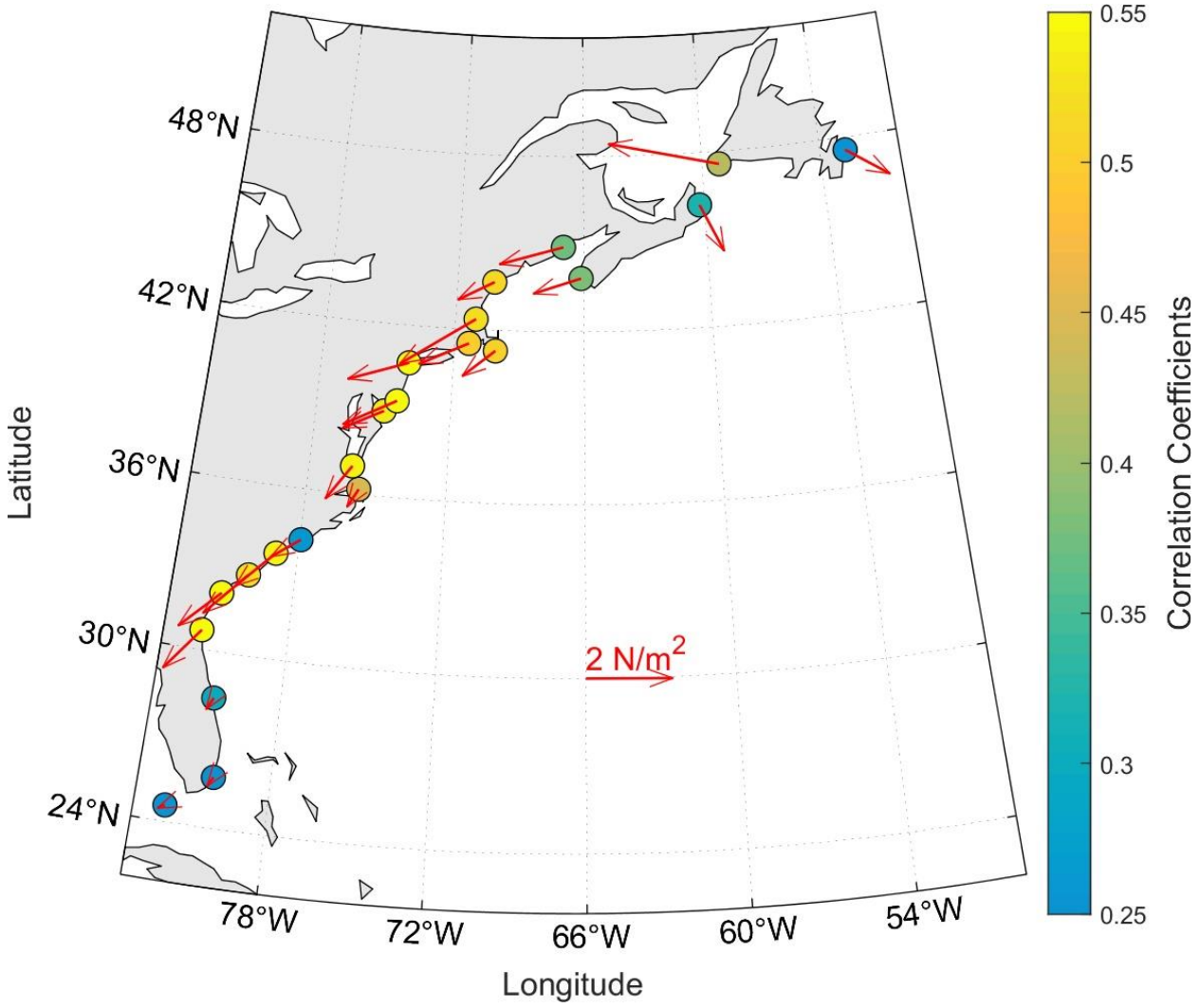

Figure S5: Arrows give the wind stress associated with one standard deviation increase of sea level at each tide gauge. These are calculated by regressing the zonal and meridional wind stress on sea level at the gauge independently and then multiplying the coefficient of the linear term by the standard deviation of the sea level. The colored dots indicate correlation coefficients between sea level and local wind stress in the directions shown by the arrows. All correlations shown are significant at the 95% level.

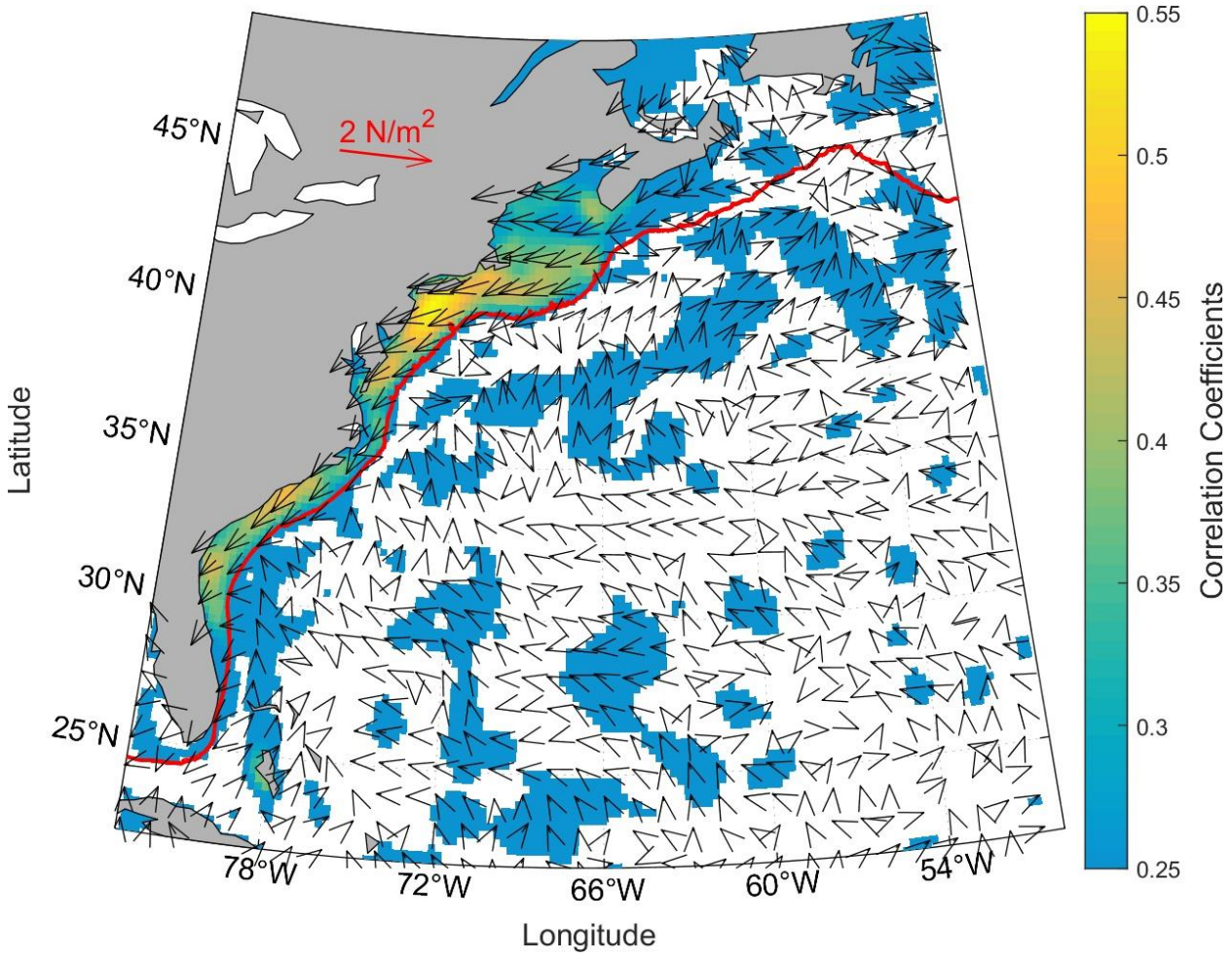

Figure S6: Arrows give the wind stress associated with one standard deviation increase of sea level at each grid point. These are calculated by regressing the zonal and meridional wind stress on sea level at the gauge independently and then multiplying the coefficient of the linear term by the standard deviation of the sea level. The background shading indicates correlation coefficients between sea level and local wind stress in the directions shown by the errors. Only correlations significant at 95% level are shown. The shelf is marked by 200-meter isobath (red line).

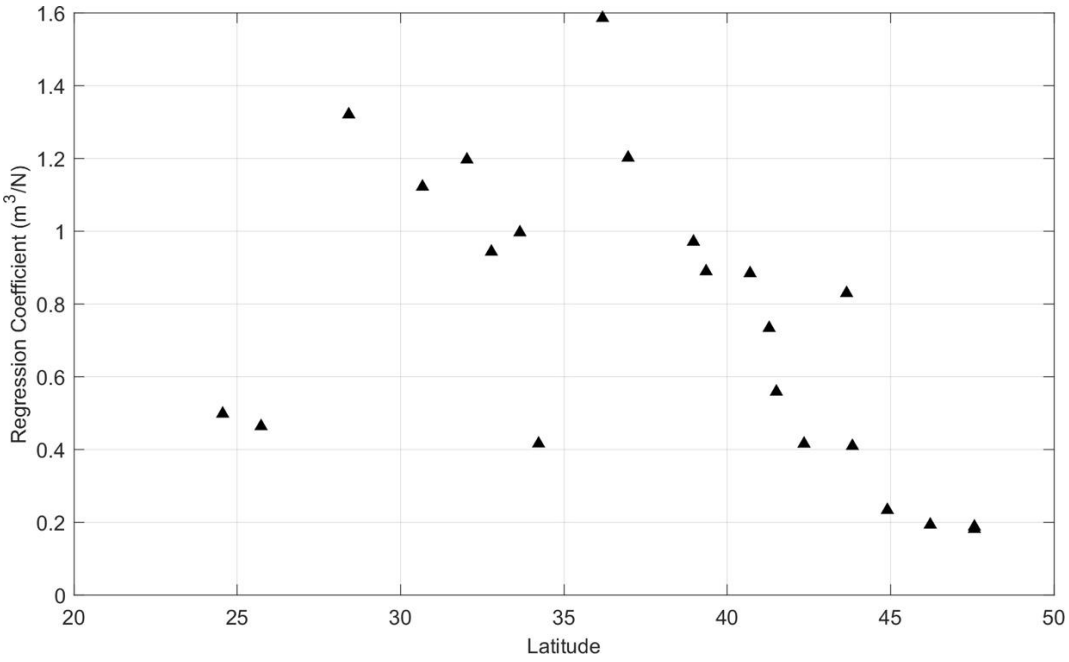

Figure S7: Regression between alongshore wind stress and sea level at tide gauges. The x-axis indices latitude of tide gauges and the y-axis indicates regression coefficients.

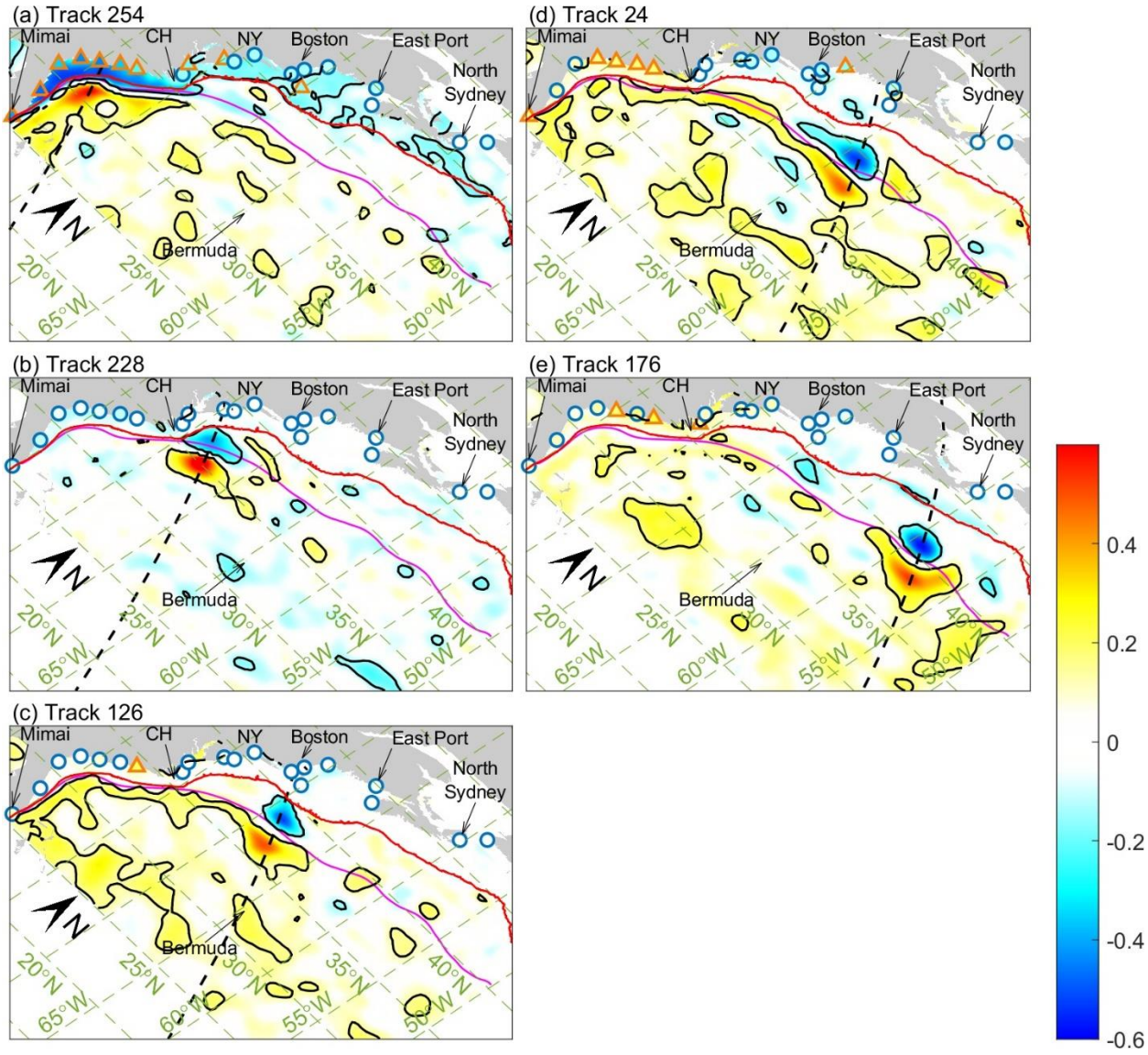

Figure S8: Same as Figure 3 but for the GS transport at the other tracks.

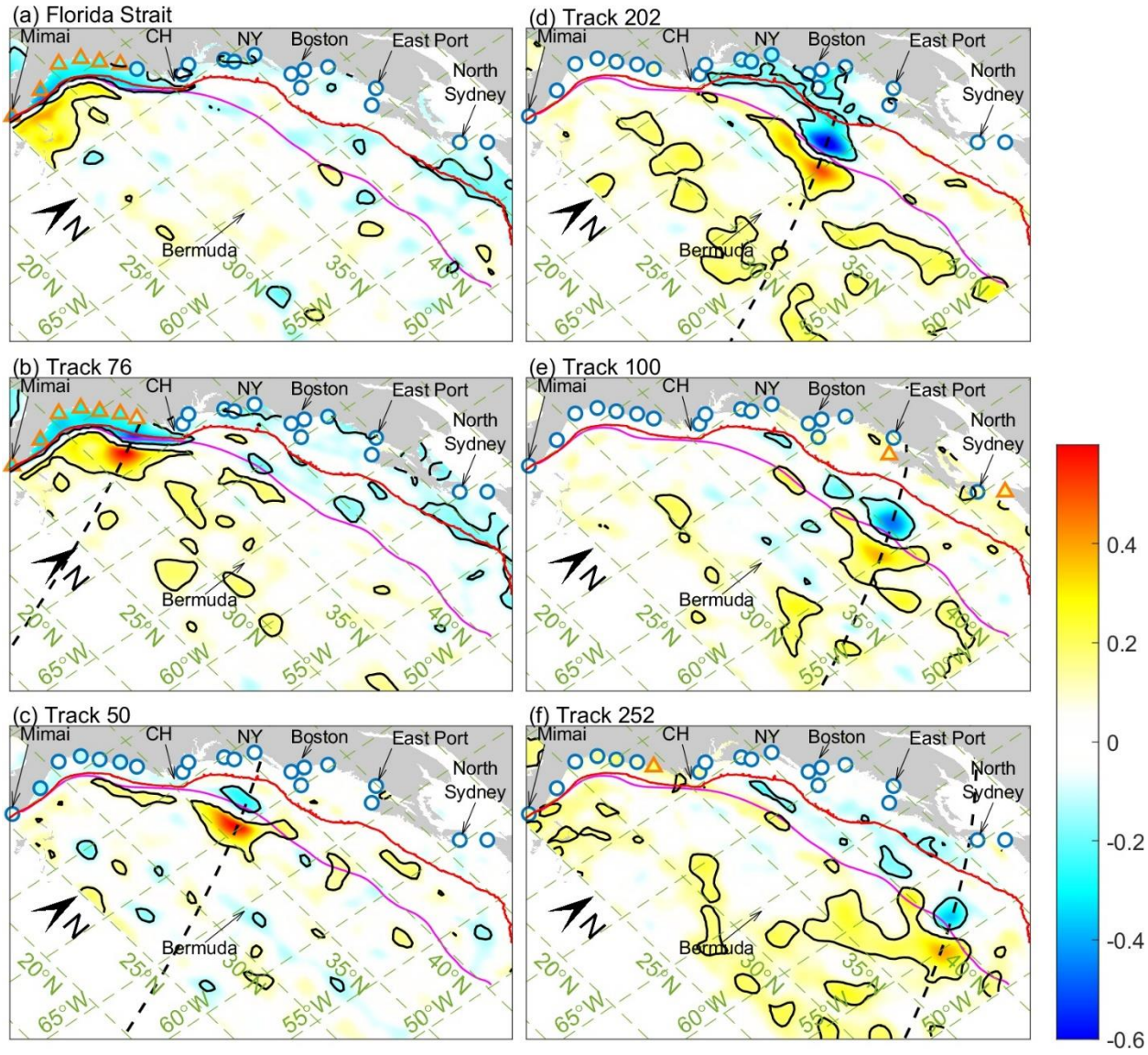

Figure S9: Same as Figure 3 but for residual sea level with local wind effects removed from both tide gauges and gridded sea level (see Text S2 for details about how local wind effects on sea level are determined). Note that local wind effects are not removed from GS transport.

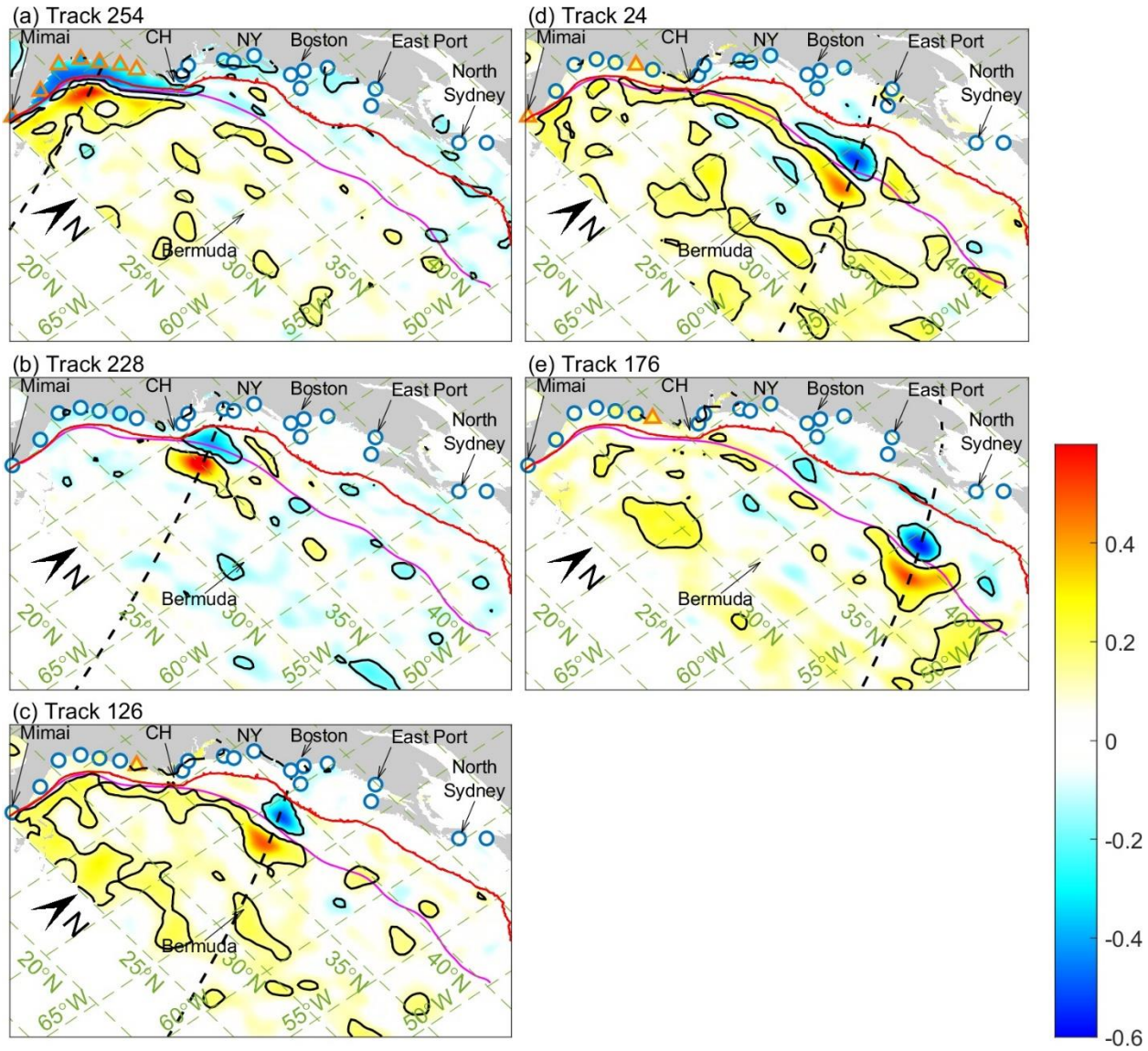

Figure S10: Same as Figure S9, in which local wind effects have been removed, but for the GS transport at the other tracks.

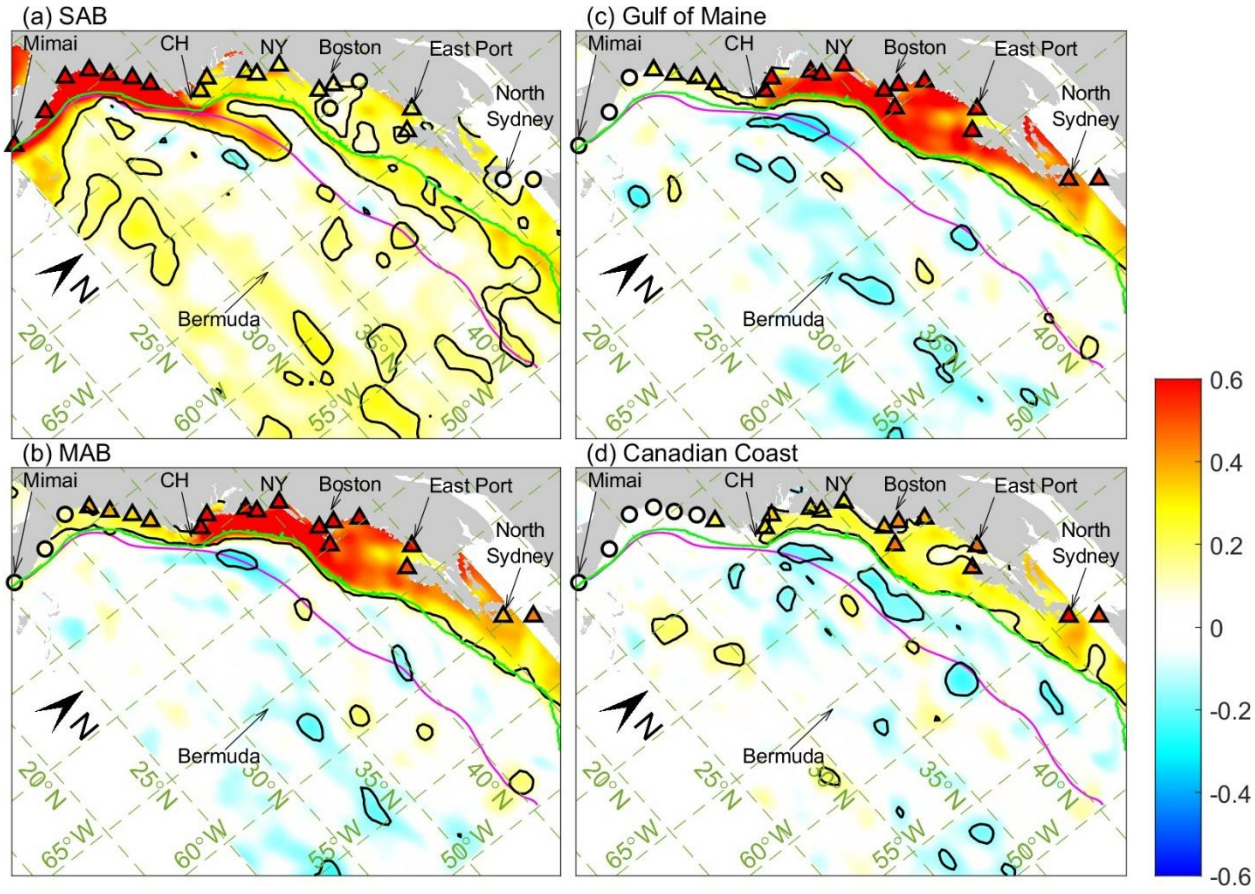

Figure S11: The shading colors indicate correlations between mean sea level from tide gauges in the (a) SAB, (b) MAB, (c) GoM, (d) Canadian Coast and gridded sea level from altimetry. Locations of the tide gauges are marked by triangles. Effects from local winds have been removed before the calculation. Significant correlations at 95% are bounded by black contours. The violet line indicates the mean GS path, and the red solid line indicates 200-meter isobath.

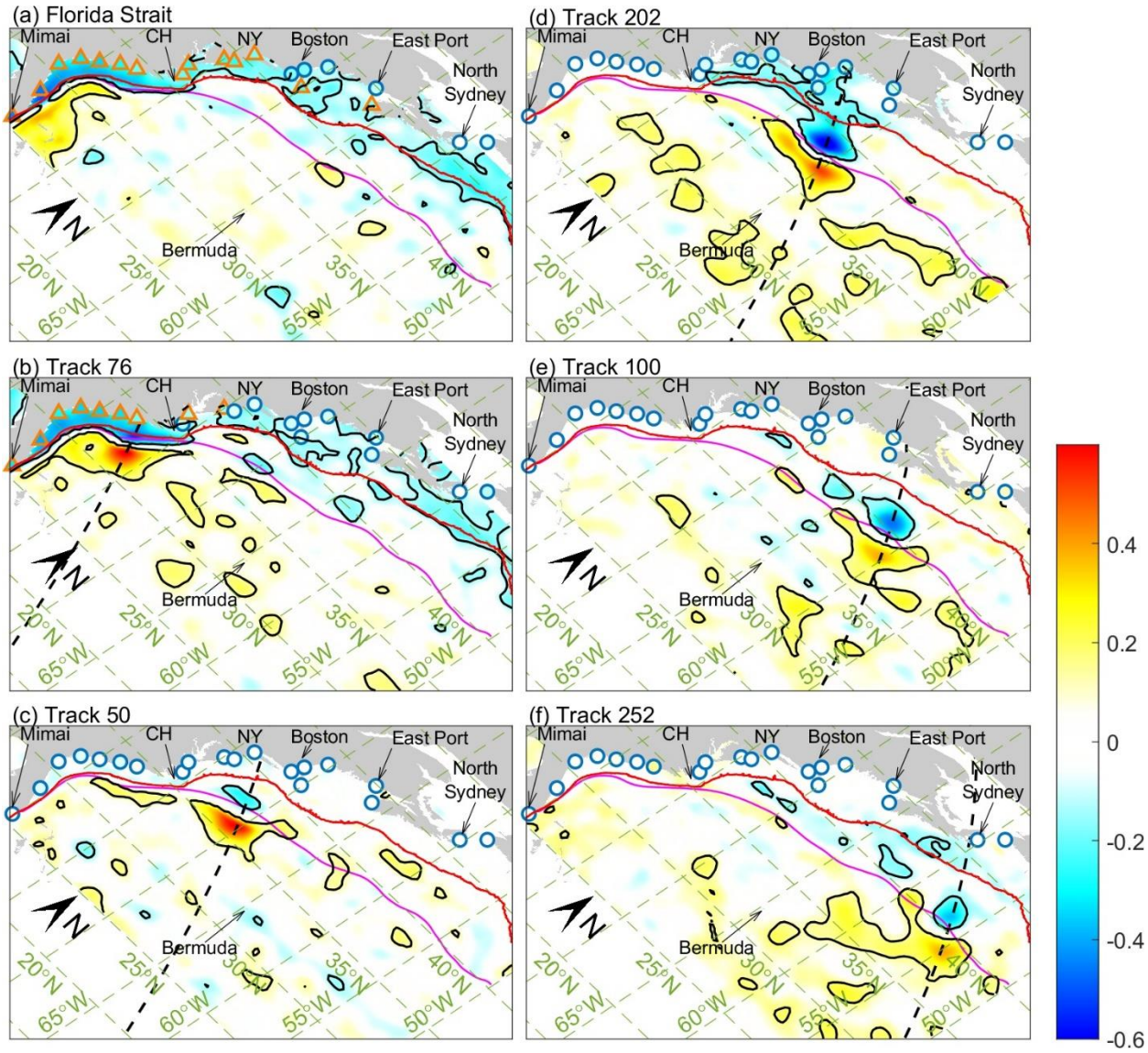

Figure S12: Same as Figure 3 but the global mean sea level is subtracted from gridded and tide gauge sea levels. The data are not detrended before the calculation since the global mean sea level has been removed.

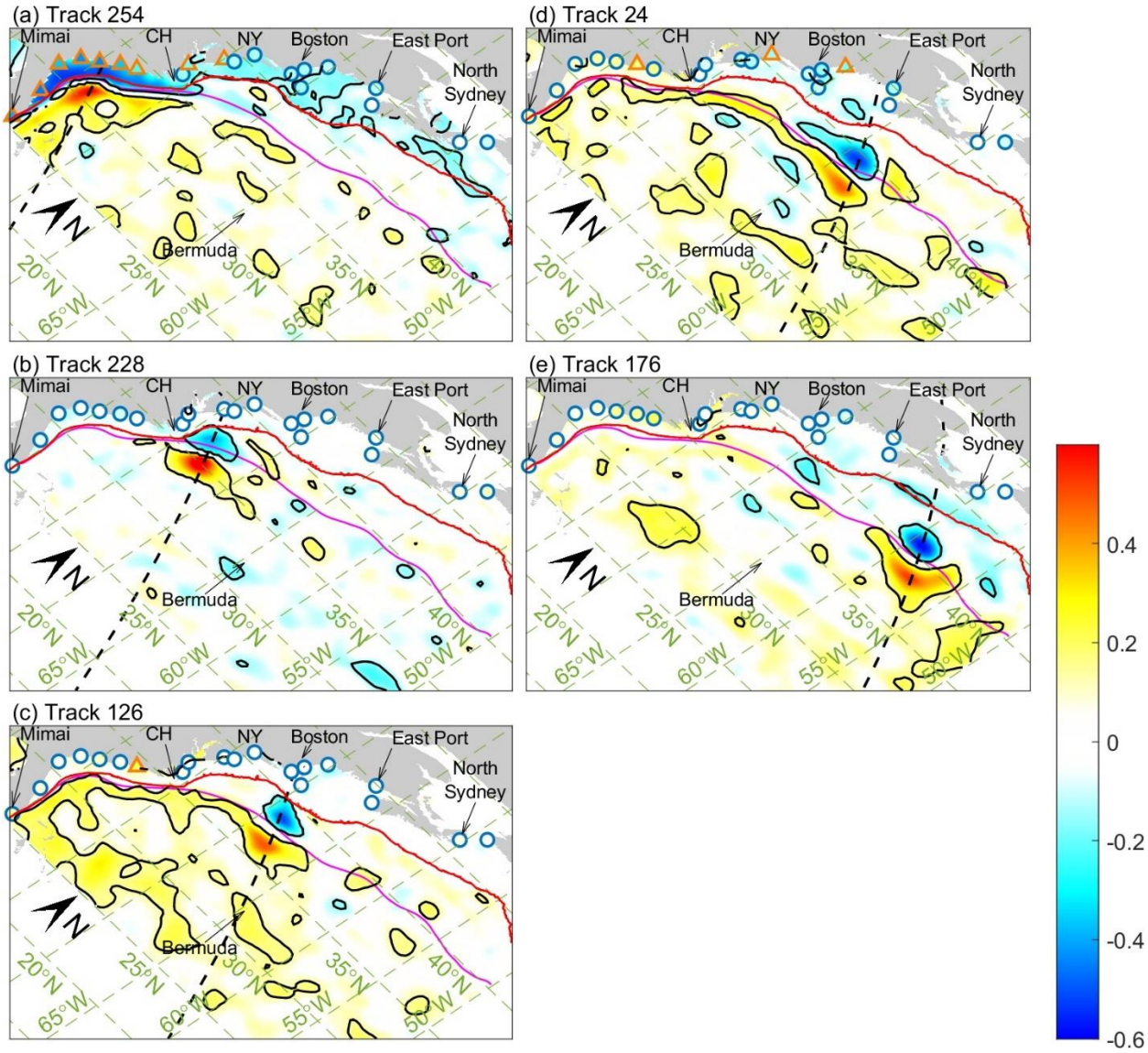

Figure S13: Same as Figure S12 but for the GS transport at the other tracks.

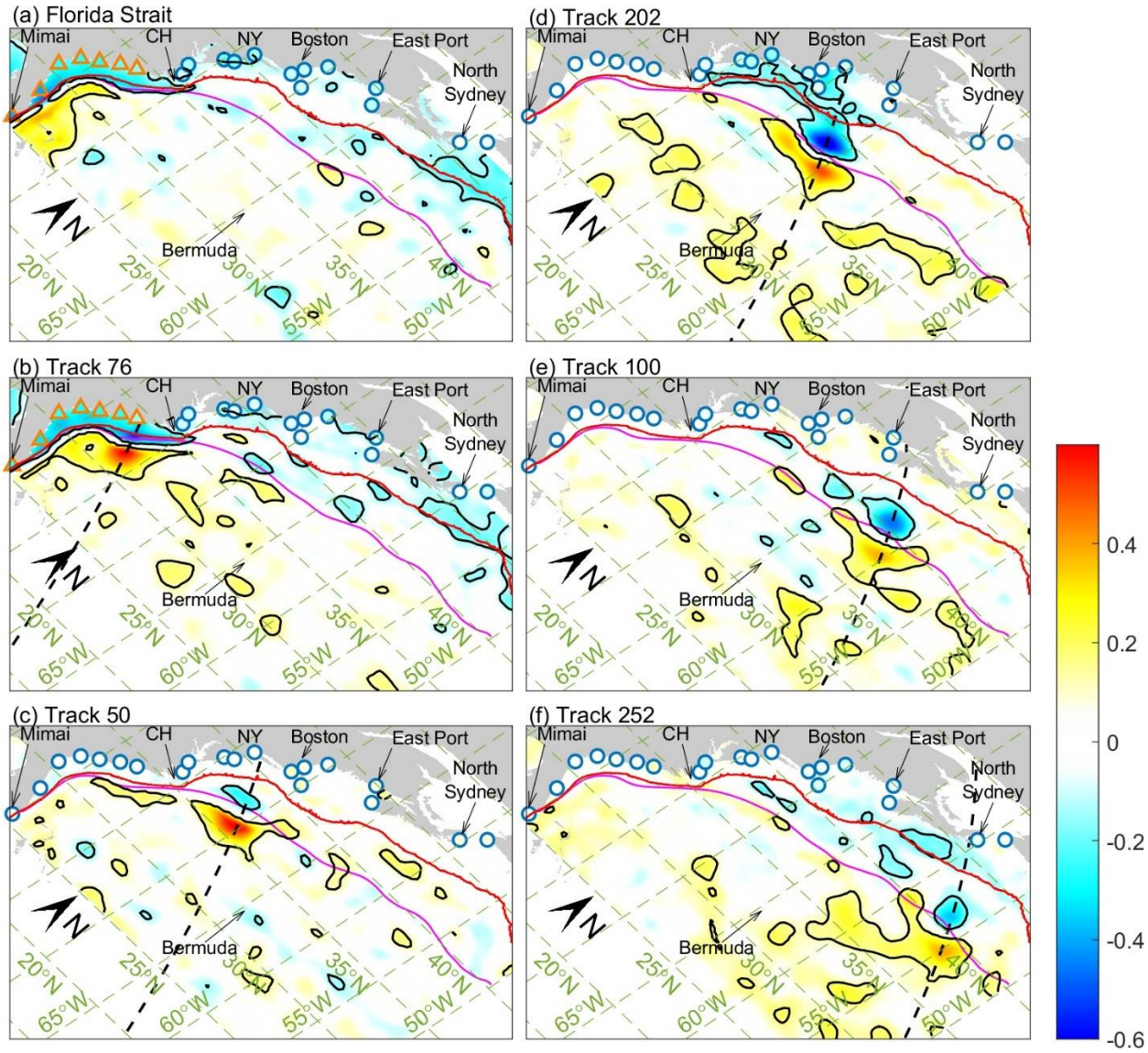

Figure S14: Same as Figure S9 but the global mean sea level is subtracted from gridded and tide gauge sea levels. The data are not detrended before the calculation since the global mean sea level has been removed.

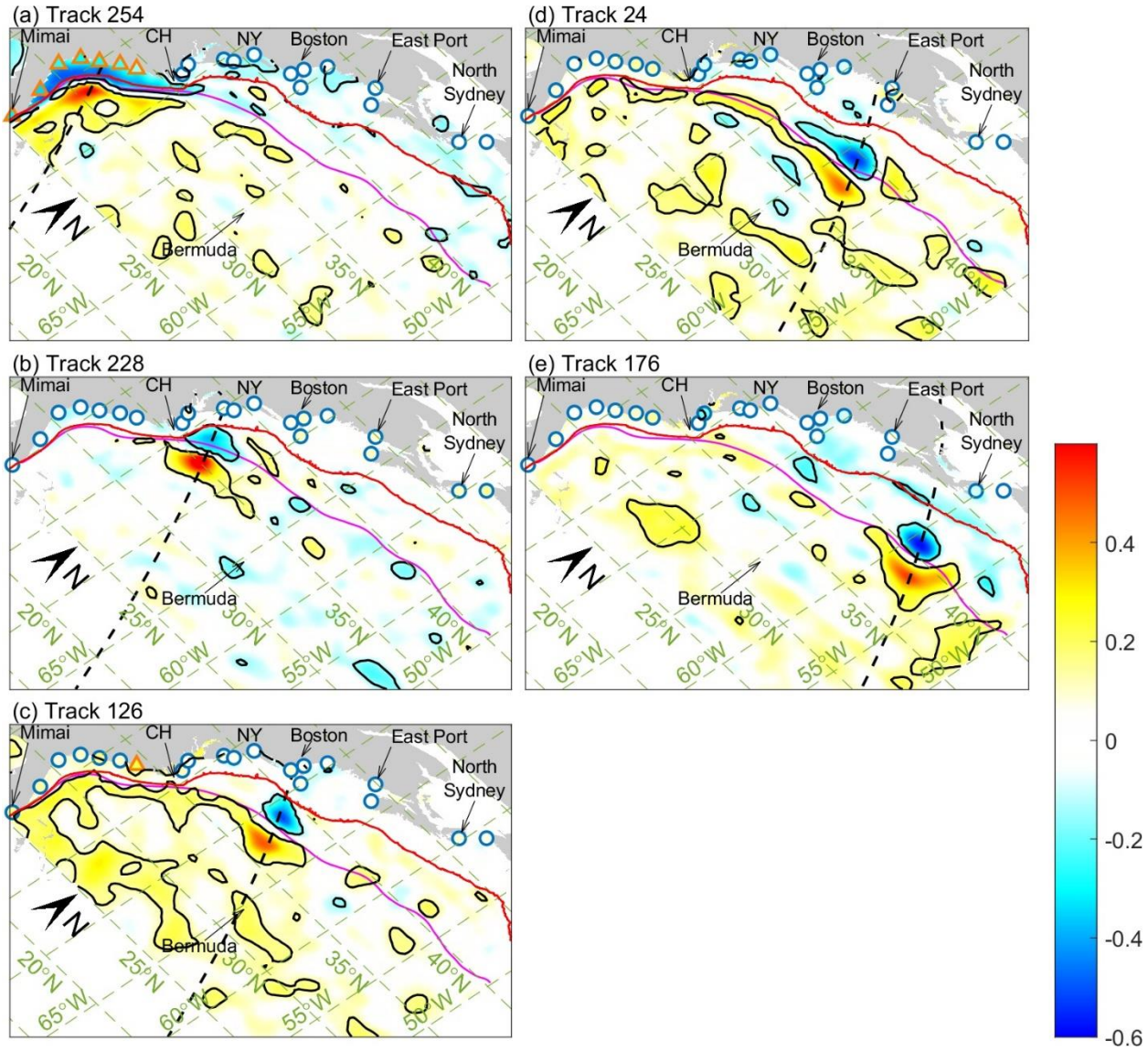

Figure S15: Same as Figure S14 but for the GS transport at the other tracks.

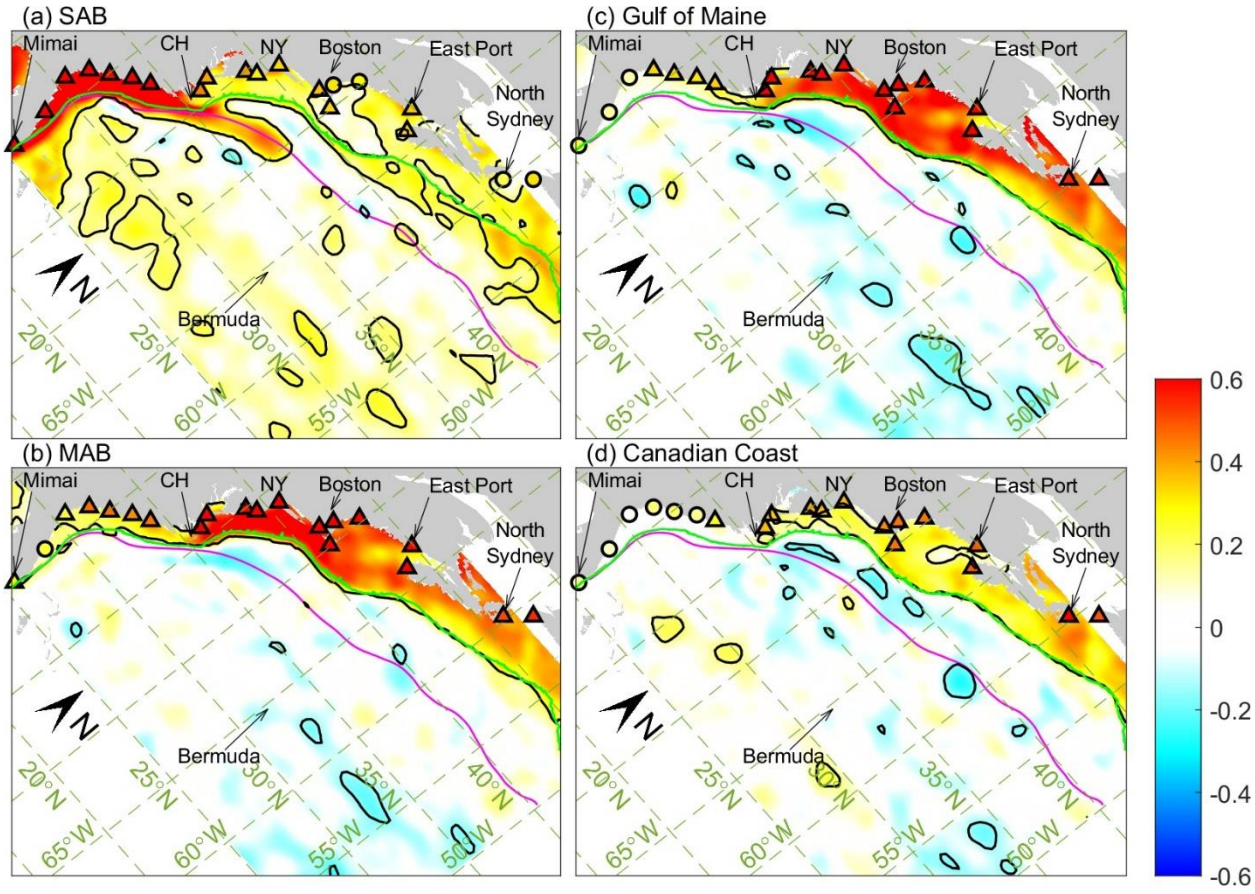

Figure S16: Same as Figure S7 but the global mean sea level is subtracted from gridded and tide gauge sea levels. The data are not detrended before the calculation since the global mean sea level has been removed.